Hydrogen bonding in methanol clusters probed by inner-shell photoabsorption spectroscopy in the carbon and oxygen K-edge regions

Y. Tamenori[1], K. Okada[2], O. Takahashi[2], S. Arakawa[2], K. Tabayashi[2], A. Hiraya[3], T. Gejo[4], and K. Honma[4]

[1] *Japan Synchrotron Radiation Research Institute/SPring-8, 1-1-1 Kouto, Sayo, Hyogo 679-5198, Japan*
[2] *Department of Chemistry, Hiroshima University, Higashi-Hiroshima, Hiroshima 739-8526, Japan*
[3] *Department of Physical Science, Hiroshima University, Higashi-Hiroshima, Hiroshima 739-8526, Japan*
[4] *Department of Material Science, University of Hyogo, 3-2-1 Kohto, Kamigori, Hyogo 678-1297, Japan*

Abstract

Hydrogen bonding in methanol clusters has been investigated by using inner-shell photoabsorption spectroscopy and density functional theory (DFT) calculations in the carbon and oxygen K-edge regions. The partial-ion-yield (PIY) curves of $H(CH_3OH)_n^+$ were measured as the soft X-ray absorption spectra of methanol clusters. The first resonance peak in the PIY curves, which is assigned to the σ*(O–H) resonance transition, exhibits a 1.20-eV blue-shift relative to the total-ion-yield (TIY) curves of molecular methanol in the oxygen K-edge region, while it exhibits a shift of only 0.25 eV in the carbon K-edge region. Decreased intensities of the transitions to higher Rydberg orbitals were observed in the PIY curves of the clusters. The drastic change in the σ*(O–H) resonance transition is interpreted by the change in the character of the σ*(O–H) molecular orbital at the H-donating OH site due to the hydrogen-bonding (HB) interaction.

I. Introduction

Inner-shell photoabsorption spectroscopy is widely used as a sensitive tool to investigate the structural and electronic properties of atoms and molecules,[1] and has been applied not only to atoms and molecules in the gas phase but to those adsorbed on surfaces. This technique has also been applied to gas-phase clusters, which bridge the gap between isolated molecules and molecules in the condensed phase.[2] Special attention has been paid to the resonance features appearing in the pre-edge regions, which are due to transitions to unoccupied orbitals that are spatially extended and strongly perturbed by the surrounding molecules. Inner-shell photoabsorption spectroscopy of clusters is thus expected to provide information about how the electronic and geometric structures of molecules change from the isolated to the condensed-phase conditions.

Since hydrogen-bonding (HB) clusters provide a unique opportunity to investigate the properties of HB under isolated conditions, they have received much attention from both experimental and theoretical viewpoints.[3] One of the most typical HB systems is water, and it is well known that the inner-shell excitation spectra of a water molecule, liquid water, and ice differ drastically.[4] Recently, this drastic change in the inner-shell excitation spectra was explained by the change in the electronic structure due to the HB interaction.[5,6,7,8,9] Two different types of OH groups exist in the HB interaction of water: H-donating OH groups and non-H-donating OH groups, i.e., free OH groups. Based on density functional theory (DFT) calculations, the difference between liquid water and ice could be related to the presence of free OH groups in liquid water.[6,7] When both the OH groups of a molecule participate in H-donating interactions, there is a loss of pre-edge features. Björneholm and coworkers have measured the inner-shell photoabsorption spectra of isolated water clusters.[10] Because of the difficulty in generating water clusters of a specific size, they measured the partial ion yield (PIY) spectra of $H(H_2O)^+$ and $H(H_2O)_2^+$ under conditions in which the average sizes of the clusters were specified. Up to an average size of 20, they observed the pre-edge structures, which were attributed to the transitions from O 1s to $4a_1$ and $2b_2$-related orbitals, though the peaks were shifted to higher energies and the intensities became weak with

increasing average size. This less drastic change in the photoabsorption spectra of water clusters is reasonable because molecular water has both H-donor and H-acceptor sites and only a fully developed HB network can have all OH groups in H-bonded state. Several free OH groups still remain in the water clusters, and the pre-edge features appear in the photoabsorption spectrum.

In contrast to the water cluster, an alcohol cluster is a more favorable system for experimental investigations on the influence of HB interactions monitored in the photoabsorption spectrum. Because each alcohol molecule has only one OH group, small alcohol clusters, whether in a ring or chain structure, have few free OH groups and, hence, a drastic change is expected in their pre-edge features. Recently, we studied the inner-shell excitation spectrum of ethanol clusters at the O K-edge and observed drastic changes in the spectrum compared with that of molecular ethanol.[11] In the pre-edge region, the first resonance excitation to the 3sa′ unoccupied orbital, which is one of the characteristic features in the absorption spectrum of molecular ethanol, was scarcely observed in the partial ion yield spectra of cluster ions. The absence of this resonance feature suggested that few free OH groups remained, even in small ethanol clusters. We clearly demonstrated that the X-ray absorption spectra of hydrogen-bonded clusters are very sensitive to changes in the electronic structure and that it is useful to investigate the correlation between the electronic structure and HB structure of the clusters.

In the present research, we extend our investigation to the inner-shell excitation of methanol clusters with a higher resolution. A theoretical approach is also employed to clarify the origin of the spectral changes between single molecules and clusters. In particular, we focus on the changes in the electronic structure at the two different sites (H-donating OH group and non-H-donating OH group) in the methanol cluster. The simple structure of methanol makes it possible to perform accurate theoretical calculations including the HB interaction. In addition, the comparison of spectra obtained in the carbon and oxygen K-edge regions is also an interesting subject. Since HB is a local interaction around

the OH site, it is expected that the influence of the HB interaction appears differently at the carbon and oxygen edges. The simple composition of methanol is, thus, more suitable for a comparison of the photoabsorption spectra obtained at carbon and oxygen K-edges. The changes in electronic structure due to HB interaction are discussed based on the experimentally and theoretically determined photoabsorption spectra in both the carbon and oxygen K-edge regions.

II. Experimental

Experiments were carried out at the soft X-ray photochemistry beamline (BL27SU) in the SPring-8 facility.[12] The light source was the radiation from a Figure-8 undulator, which can produce a linearly polarized photon beam.[13] The photon beam was dispersed by a soft X-ray monochromator with varied-line-spacing plane-gratings and then introduced into the ionization region of a coincidence measurement instrument. The photon energy resolution during the measurements was set at 30 meV (carbon K-edge region) or 60 meV (oxygen K-edge region). The experimental apparatus was divided into two parts: a nozzle chamber and a main chamber. Each chamber was evacuated by a wide-range turbo-molecular pump (SHIMADZU, TMP2303LMC) with a rated pumping speed of 2000 L/s. The background pressures of the nozzle and main chambers were typically 3×10^{-6} and 1×10^{-6} Pa, respectively. In the main chamber, the molecular beam was crossed with a soft X-ray beam (0.1 × 0.2 mm) in the ionization region of a double-field-type time-of-flight (TOF) mass spectrometer.[14] The ions and electrons formed by the soft X-ray absorption were extracted toward opposite directions in the ionization region. The electrons were detected by a micro-sphere-plate (MSP, El-Mul) and the ions were detected by another MSP after the flight through the TOF tube. The electron signals were fed to the start pulse input of a multi-stop time-to-digital converter (FAST ComTec, 7886) and the ion signals were fed to the stop pulse input to obtain photoelectron-photoion coincidence (PEPICO) signals.

Methanol clusters were produced by a seeded beam method. Helium at pressure of 2 atm was bubbled through a sample reservoir containing a liquid sample at room

temperature (27 °C), and the mixture was expanded through a nozzle of 30 μm in diameter. The supersonic beam was collimated by a skimmer (Beam Dynamics, 1.0 mm dia.) and introduced into the main chamber. The mean cluster size was estimated as less than 50, referring to a previous report.[15] During the measurements, the pressures of the nozzle and main chambers were around 2×10^{-2} and 4×10^{-4} Pa, respectively.

For a comparison with the inner-shell photoexcitation spectra of clusters, the spectra of molecular methanol were measured under an effusive beam condition. For this measurement, pure sample vapor was directly introduced through a 1/16-in (outside diameter) needle into the ionization region. The pressure in the main chamber was 4×10^{-4} Pa during the effusive beam measurement. Methanol (purity > 99.9%) was obtained from Wako Pure Chemical Industries, Ltd. Helium gas with a stated purity of 99.99% was purchased from Taiyo Toyo Sanso Co., Ltd.

III. Theoretical Methods

Geometry optimizations of methanol and methanol clusters were carried out using the GAUSSIAN 03 program[16] at the B3LYP/cc-pVTZ level of approximation. The basis set superposition error (BSSE) was corrected by the counterpoise method at each setup of the optimization of each cluster.

The X-ray photoabsorption spectra calculations were performed using the StoBe-deMon program[17]; the detailed computational method has been described in previous reports.[18,19,20] In brief, the theoretical X-ray photoabsorption spectra were generated by the transition potential (DFT-TP) method.[21] The gradient-corrected exchange (PD86)[22] and correlation functionals (PD91)[23] established by Perdew and Wang were applied. The orbitals for the species in the excited states were determined using a molecular basis set with a half-occupied core orbital at the ionization site. The orbitals for the excited electron were then obtained by diagonalizing the Kohn–Sham matrix built from the density with the basis set extended by a large set of diffuse basis functions centered on the excited atom. The

obtained orbital energies and computed transition moments provide the excitation energy and associated intensities in the theoretical spectrum. The DFT-TP calculation of the spectrum corresponds to the static exchange approach and, thus, neglects the relaxation effect of the created ion core by adding the excited electron. This effect is largest for valence-like excitations and, thus, these states were computed with fully-relaxed ΔKohn–Sham calculations.[24] For a more accurate estimate of the absolute excitation energy, relativistic and functional corrections were added to the excitation energy.[18] The relativistic corrections added to the ionization potential were 0.08 eV and 0.33 eV for the C and O K-edges, respectively. The non-core-excited atoms were described by effective core potentials.[25] Finally, the spectra were generated by a Gaussian convolution of the discrete lines by varying the broadenings. The computed C K-edge spectra were broadened using Gaussian functions with a constant width of 0.5 eV below 289 eV, then linearly increasing up to 4.5 eV at 297 eV. The computed O K-edge spectra were broadened using Gaussian functions with a constant full width at half maximum (FWHM) of 0.5 eV below 537 eV, then linearly increasing up to 4.5 eV at 549 eV.

IV. Results and discussion

A. TOF mass spectra of molecular and cluster methanol

The PEPICO spectra were measured to study the yield of ionic species formed by the soft X-ray absorption. The PEPICO spectra were then converted to the TOF mass spectra, as shown in Fig. 1. The spectra were measured under (a) seeded supersonic beam (He 2 atm) and (b) effusive beam conditions. The spectra were recorded at a photon energy of 545.0 eV, which is above the O 1s ionization threshold of methanol (539.1 eV).[26] The spectra of both individual methanol molecules and clusters obtained in this study are in agreement with those reported in previous studies.[15,27] Under the effusive condition, ions larger than the parent methanol ion (m/z = 32) were not seen in the mass spectrum.

On the other hand, under the seeded supersonic beam condition, several ions with

$m/z \geq 32$ were observed (Fig. 1(a)). These peaks are assigned to protonated methanol cluster ions, $H(CH_3OH)_n^+$ (n = 1–4), which have also been detected in previous experiments in the vacuum ultraviolet (VUV)[28] and soft X-ray regions.[15] Primarily formed inner-shell excited or ionized methanol clusters presumably suffer from extensive fragmentation and, hence, convert to energetically stable protonated clusters, $H(CH_3OH)_n^+$, as already proposed in a multiphoton ionization study.[29] The relative intensities of small fragment ions (m/z < 32) observed in the seeded beam are almost identical to those obtained in the effusive one. This indicates that the major component of the small fragment ions can be assumed to be originating from the fragmentation of molecular methanol.

B. Experimental photoabsorption spectra of methanol in the O K-edge region

Figure 2 shows the photoabsorption spectra of methanol and methanol clusters measured in the O 1s region. The energy resolution of the photon beam was set at 60 meV. The photoabsorption spectrum of molecular methanol was measured under the effusive beam condition using a TIY method. The TIY spectrum obtained in the present study is almost identical to those reported by earlier investigations.[26,27,30,31] The assignment of each peak in accordance with the results of previous studies is given in Fig. 2(a). The photoabsorption spectra of methanol clusters were measured under the seeded supersonic molecular beam condition (He 2 atm) and extracted as PIY spectra from the peak areas of protonated clusters in the TOF mass spectra acquired as a function of the photon energy. Under the seeded supersonic beam condition, protonated methanol clusters up to $H(CH_3OH)_4^+$ were observed, as seen in Fig. 1(a). In Fig. 2, the PIY curves of $H(CH_3OH)_n^+$ for n = 1–3 are shown.

Although the $H(CH_3OH)_n^+$ PIY curves are quite similar, indicating cluster size independent absorption cross section for the neutral $(CH_3OH)_x$ parent clusters, they show drastically different features than those of the TIY curve measured under the effusive beam condition. The differences are summarized as follows:

(1) The peak at 534.07 eV in the TIY curve of methanol is strongly suppressed in the PIY

curves of $H(CH_3OH)_n^+$ and a small hump appears at 535.27 eV, instead.

(2) The peak at 537.12 eV (3pa′) in the TIY curve is suppressed and becomes a shoulder in the PIY curves.

(3) At higher energies, the valley between the higher Rydberg region (538.0 eV) and the σ*(C–O) resonance maximum (540.1 eV) disappears in the PIY curves.

Prince *et al.* assigned the first resonance peak at around 534 eV to the orbital with O–H anti-bonding characteristics.[26] From the calculated orbital contour plots for methanol, Wilson *et al*. supported that the first resonance peak can be assigned to the σ*(O–H) orbital with some contribution from the p orbital on the C-atom.[31] Therefore, difference (1) is likely to be ascribed to a drastic change in the σ*(O–H) orbital. Since the peak at 537.12 eV is assigned to the 3pa′ resonance excitation, difference (2) could be responsible for the change in this orbital in the methanol clusters. Difference (3) can be interpreted by the suppression of transitions to higher Rydberg states at around 538 eV as well as by an apparent red-shift of the σ*(C–O) resonance maximum. These differences must be attributed to the characteristics of the methanol clusters: since the most important interaction in the methanol clusters is HB, the drastic change in the resonance features should be explained by the HB interaction. For a greater understanding of the experimental photoabsorption spectra, a theoretical approach using DFT calculation was applied.

C. Theoretical photoabsorption spectra of small methanol clusters as a model system

In the present study, we performed DFT calculations for the ring and chain methanol trimers as the smallest model systems. The optimized structure for the most stable methanol trimer is a ring structure; the formation of a cyclic structure maximizes the number of hydrogen bonds in the clusters. This result is consistent with those of previous investigations.[32,33] However, in order to elucidate the changes in the photoabsorption spectrum at different OH sites, DFT calculations for a chain methanol cluster were also performed. The chain trimer is the simplest system having three different sites, i.e., a

terminal H-donor, a terminal H-acceptor, and an interior molecule that donates the H atom to the H-acceptor and receives an H atom from the H-donor. For the calculation of the chain cluster, we chose an open-ring structure in which one HO…H bond is broken in the optimized ring structure. Several minima exist on the potential energy surface for the methanol trimer, and the open-ring structure is one of them. Although the open-ring structure is not the most stable, it is a suitable structure for comparison with the photoabsorption spectrum of the ring trimer since it can minimize the unfavorable effects of geometrical change on the photoabsorption spectrum.

Figures 3A and 3B show the calculated photoabsorption spectra of the chain (3A) and ring trimers (3B) in the O K-edge region. The calculated spectrum of a methanol monomer is also shown at the top of each figure. In Fig. 3A, the contributions of the H-acceptor, interior, and H-donor components as well as the sum of the three components are shown in Fig. 3A(b–e). Similarly, the contributions of the three methanol components (b–d) are separately indicated in Fig. 3B, while their sum is shown at the bottom. The spectrum of the H-acceptor [Fig. 3A(b)] is very similar to the monomer spectrum, except for the slight shift to the higher-energy side. The shift of the peaks can be explained based on the change in the electron density due to the HB interaction: the H-acceptor provides the lone-pair electrons on the O atom due to the HB interaction, and the decreased electron density leads to the blue-shift in the photoabsorption spectrum. On the other hand, the spectra of the (c) interior and (d) H-donor molecules are remarkably different from the monomer spectrum. In Fig. 3A(c), the first peak at about 534.4 eV in the monomer spectrum is absent and a new peak appears at about 534.8 eV. The second peak of the monomer spectrum is shifted to the lower-energy side in (c). The third peak loses its intensity and is slightly shifted to the lower-energy side, while a large, broad band appears across the ionization threshold (539 eV). The spectrum of the H-donor methanol shows changes similar to those of the interior molecule and a rather larger energy shift as compared to that of the H-acceptor methanol. Moreover, the spectrum obtained for the ring trimer also shows very similar changes in the

interior and H-donor spectra of the chain trimer. The theoretical results indicate that the OH groups in the methanol cluster can be classified into two groups, i.e., the H-donating OH groups and the non-H-donating OH groups. The changes of the photoabsorption spectrum can be related to the presence of hydrogen donation. This is consistent with the results of previous investigations on liquid water and ice.[5,6,7,8,9]

The difference between the calculated monomer and H-donating spectra is parallel in trend to the observed difference between the TIY and PIY spectra. The two observed broad bands in the pre-edge region can be interpreted as follows, based on this trend: the first σ*(O–H) resonance in the TIY spectrum is slightly shifted to the higher-energy side in the PIY spectra, whereas the second resonance is shifted to the lower-energy side. The first band observed at 535.3 eV in the PIY spectra could be assigned to these two overlapped components. The second band at about 537.1 eV has mainly a 3pa′ character. The similarity between the calculated H-donating spectra and the experimental PIY spectra indicates that almost all of the OH groups in the cluster donate their H atoms, and the σ*(O–H) orbital, which is responsible for the first resonance excitation, is expected to change drastically due to the H donation. This result is also consistent with that of infrared (IR) studies on methanol clusters, which have shown that neutral methanol clusters larger than dimers have cyclic structures.[32] When methanol clusters form a ring structure, every hydrogen atom in the OH groups should be donated to create a hydrogen bond.

The drastic spectral change at the first resonance peak can be interpreted in terms of the change in the molecular orbitals. Figure 4 shows the molecular orbitals responsible for the resonance excitation of the monomer, H-acceptor, interior, and H-donor methanol molecules in the open-ring trimer. The σ*(O–H) orbital has a strong dissociative character in molecular methanol, as shown in “Monomer” in Fig. 4. Among the three molecular orbitals of the open-ring trimer shown in Fig. 4, the orbital of the H-acceptor is quite similar to that of the monomer. This similarity is consistent with the similarity of the absorption spectrum of the H-acceptor with that of molecular methanol. However, the orbitals of the

H-donor and interior molecules change drastically from that of the monomer. The large lobe on the H atom in the O–H bond is shrunk due to the interaction with the H-acceptor molecule. Also discernible is the electron cloud around the O atom in the H-accepting methanol. This molecular orbital indicates the interaction between the σ*(O–H) orbital of the H-donor and a p orbital of the O atom in the H-acceptor through HB. The formation of the new molecular orbital due to the HB interaction shifts the peak position to the higher-energy side, and the reduced amplitude around the OH site decrease the peak intensity.

The cluster formation also affects the pre-edge features originating from the transitions to the higher Rydberg orbitals (Fig. 2). Although it is difficult to discuss the change in each transition due to the unresolved broad band, the observed spectral change is considered to be reasonable. Since the Rydberg orbitals generally have large radii, their characters are affected by interactions with adjacent atoms or molecules. It has been reported that the transition to molecular Rydberg states becomes broader and peaks shift toward higher energies in several rare-gas matrices.[34] Since the HB interaction is rather strong as compared with van der Waals or dipole-type interactions, the Rydberg orbitals are likely to shift their energies to the higher values and also change their absorption intensities. The HB interaction affects the change in the molecular orbital shape in the vicinity of the O atom in the H-donor, and thereby causes changes of the photoabsorption spectrum.

D. Photoabsorption spectra of methanol cluster in the C K-edge region

Figure 5 shows the photoabsorption spectra of methanol measured in the C 1s region under effusive beam and seeded supersonic molecular beam conditions (He 2 atm). Some changes can be clearly seen in the cluster spectra: First, the first resonance corresponding to the σ*(O–H) peak is shifted to the higher-energy side by about 0.25 eV from that for the methanol molecule (287.96 eV). Second, the σ*(C–H)/3pa″ resonance (289.44 eV) is shifted to the lower–energy side. Finally, the Rydberg peaks separated clearly in the TIY from the monomer are hardly resolved in the PIY curves from the methanol clusters. The

unresolved higher Rydberg peaks shift to the lower-energy side and form a broad maximum at about 290.5 eV.

To understand these spectral changes, theoretical calculations were performed for the ring trimer at the C K-edge ; the results are shown in Fig. 6(b). The calculated spectrum of a methanol monomer is also shown in Fig. 6(a). The trimer spectrum closely resembles the monomer spectrum. The clear changes found in the spectra are the slight peak shifts: the first resonance peak is shifted to the higher-energy side, while the second peak is shifted to the lower–energy side. Also, the large, broad maximum at about 293.0 eV shifts to the lower-energy side, thereby increasing the intensity at the higher Rydberg states.

The changes observed in the theoretical spectra are in good agreement with the PIY spectra. Furthermore, the observed trend in peak shifts is consistent with that at the O K-edge. However, in contrast to the large energy shift observed at the O K-edge, the shifts observed at the C K-edge are rather small. The difference is interpreted by the localized features of the HB interaction around the OH site; thus, the influence on the carbon atom is smaller than that on the oxygen atom. This result suggests that the HB interaction operates primarily through the OH bond, and molecular orbitals around the CH_3 site experience a rather weak influence from the neighboring molecules.

E. Influence of larger clusters on the photoabsorption spectrum

The theoretical spectra of methanol trimers described in the previous sections are very useful to explain the observed differences between the $H(CH_3OH)_n^+$ PIY from the methanol cluster and the TIY of methanol monomer. That is, the HB donation causes a drastic shift in the σ*(O–H) peak, while only small shifts are expected for the non-H-donating OH groups. The resonances at the C K-edge are also expected to show small shifts. The experimental spectra shown in Figs. 2 and 5 are consistent with this expectation, i.e., that the spectral change observed at the O K-edge is more drastic than that observed at the C K-edge.

The PIY curves, even for ions as small as $H(CH_3OH)^+$, contain contributions from neutral parent clusters larger than dimers. The observed protonated clusters [$H(CH_3OH)_n^+$] can be produced from various sizes of clusters greater than *n*-mer because the excited clusters evaporate neutral fragments as well as ionic fragments. Various sizes of clusters coexist in the supersonic beam, and hence, one can only determine the average size of the clusters by controlling the experimental conditions such as the backing pressure and temperature. Therefore, the dominant features seen in the experimental PIY curves are mainly attributed to clusters larger than trimers in this study. However, the theoretical spectra of the trimer can still be used to explain the spectral changes observed. We discussed the three spectral changes in the O K-edge region in the previous section. Among the three drastic changes, the most striking is the suppression of the σ*(O–H) peak at 534.07 eV seen in the TIY curve of methanol and the appearance of the small hump at 535.27 eV in the PIY curves of $H(CH_3OH)_n^+$. This is expected for the clusters with all H-donating OH groups, as induced from the theoretical spectra of the trimer. Because only the transition from the O 1s electrons in the H-acceptor contributes the peak at 534 eV, the suppression of this peak observed in the present study clearly suggests that the clusters have ring structures where all the OHs create the H-donating interaction. The present results indicate that, even if a cluster is larger than a trimer, the change in the σ*(O–H) orbital due to the H-donating interaction is the essence behind the change in photoabsorption spectrum in the methanol cluster.

F. Comparison with the absorption spectra of liquid methanol

Liquid methanol can provide relevant information about the cluster-size dependence of the photoabsorption spectrum. The influence of HB interaction in liquid methanol has been studied from both the theoretical and experimental points of view in the inner-shell excitation region.[31,35] The electronic and geometric structures of liquid methanol have been investigated using soft X-ray emission spectroscopy by Kashtanov *et al*.[35] They concluded that liquid methanol consists of ring and chain structures dominated by six and eight

methanol units. On the other hand, Wilson *et al.* investigated the electronic structure of liquid methanol using soft X-ray photoabsorption spectroscopy,[31] concluding that the bulk liquid is comprised of chain clusters longer than 6-mer and ring clusters. In both studies, DFT calculations for small clusters were performed to interpret the experimental observations, leading to the conclusion that small clusters play an important role in liquid methanol.

The present PIY spectra are similar to the spectra of liquid methanol in both the C and O K-edge regions except for the following minor differences: In the O K-edge region, the two pre-edge features at 535.27 eV and 537.12 eV are clearly identified in the PIY spectra of clusters, while these two features are not clear in the spectrum of liquid methanol.[28,32] In the C K-edge region, the PIY curves of clusters show a clear shift in the first resonance peak, which remains as a shoulder in liquid methanol. In both cases, the PIY spectra of methanol clusters seem to show a good demonstration of the spectral change expected from the calculation.

There are two possibilities for the discrepancies between liquid methanol and isolated clusters. One possibility is the saturation of the photoabsorption spectra. The spectra of liquid methanol were measured by using the X-ray fluorescence yield or total electron yield method. Näslund *et al.* compared the photoabsorption spectra of liquid water recorded with different techniques and pointed out that the saturation effect due to different probing depths caused the minor differences, i.e., those in the spectral widths and relative intensities.[36] Since the techniques applied to liquid methanol are sensitive to the saturation effect, a part of the discrepancies may have originated from this effect.

Another possible explanation is the differences in the experimental conditions. The spectrum of liquid methanol was obtained at room temperature (~280 K). Because the energy differences between conformers of methanol clusters are estimated as being on the order of a few kJ/mol, several conformers are expected to coexist in the liquid phase.[37] The coexistence of ring and chain structures in liquid methanol has been suggested by both theoretical and experimental studies.[35] On the other hand, the methanol clusters studied

here were formed by supersonic expansion and mainly had the most stable structure under the low-temperature condition. An IR study has suggested that almost all methanol clusters have ring structures in a supersonic molecular beam.[32] The technique employed in this study is likely to provide a "ring-structure-sensitive" photoabsorption spectrum.

V. Summary

We measured the soft X-ray photoionization spectra of methanol clusters by means of the partial-ion-yield method in the C and O K-edge regions. In the PIY spectra of methanol clusters, the characteristic resonance excitation to the σ*(O–H) orbital exhibited blue-shifts of 0.25 and 1.20 eV in the C and O K-edge regions, respectively, and the transition intensity to higher Rydberg states was suppressed. This change in the photoabsorption spectrum was investigated by using DFT calculations. The model calculation for the methanol trimer clearly illustrated that the shape of the unoccupied molecular orbitals of the H-donor was changed by the interaction with the lone-pair electrons in the H-acceptor methanol. The drastic change observed at the first resonance at the O K-edge was explained by the loss of the free or acceptor-only OH site. The present study indicates that the X-ray absorption spectra of HB clusters are sensitive to the changes in the local electronic structure caused by the HB interaction and are useful in investigating the change in electronic structure from that of an isolated molecule to those of HB clusters.

Acknowledgements

This experiment was carried out with the approval of the SPring-8 Proposal Review Committee (Proposals 2002B0284-NS1-np, 2003A0677-NS1-np, 2003B0275-NS1-np, and 2006A1282). The authors would like to thank Prof. L. G. M. Pettersson for his helpful discussions. YT is grateful for the partial financial support from a Grant-in-Aid for Young Scientists (B) from the Ministry of Education, Culture, Science, and Technology of Japan (1875002). TG is grateful for the financial support of the Matsuo Academic Foundation and Hyogo Science and Technology Association.

Figure captions

Figure 1 TOF mass spectra of fragment ions: (a) seeded in 2 atm He and (b) under effusive methanol beam condition. The inset shows the expanded region of 26-35 amu. Excitation energy was 545.0 eV (above ionization threshold). The spectra were obtained using the photoelectron-photoion coincidence method and then converted to the TOF mass spectra.

Figure 2 PIY spectra of cluster ions (b–d) formed from the photoionization of a methanol beam at the oxygen K-edge. TIY of the methanol molecule is shown in panel (a).

Figure 3 Calculated photoabsorption spectra of chain (A) and ring (B) methanol trimers in the O K-edge region. Curve (a) indicates the calculated spectrum of the monomer. Curves (b) to (d) indicate the contribution of each molecule separately, and (e) is the sum of the three components.

Figure 4 (Color online) The O K-shell excited molecular orbitals corresponding to the first resonance peak shown in Fig. 3A.

Figure 5 PIY spectra of cluster ions (b–d) formed from the photoionization of a methanol beam at the carbon K-edge. TIY of the methanol molecule is shown in panel (a).

Figure 6 Calculated photoabsorption spectra in the C K-edge region of (a) methanol monomer and (b) trimer.

Figure 1

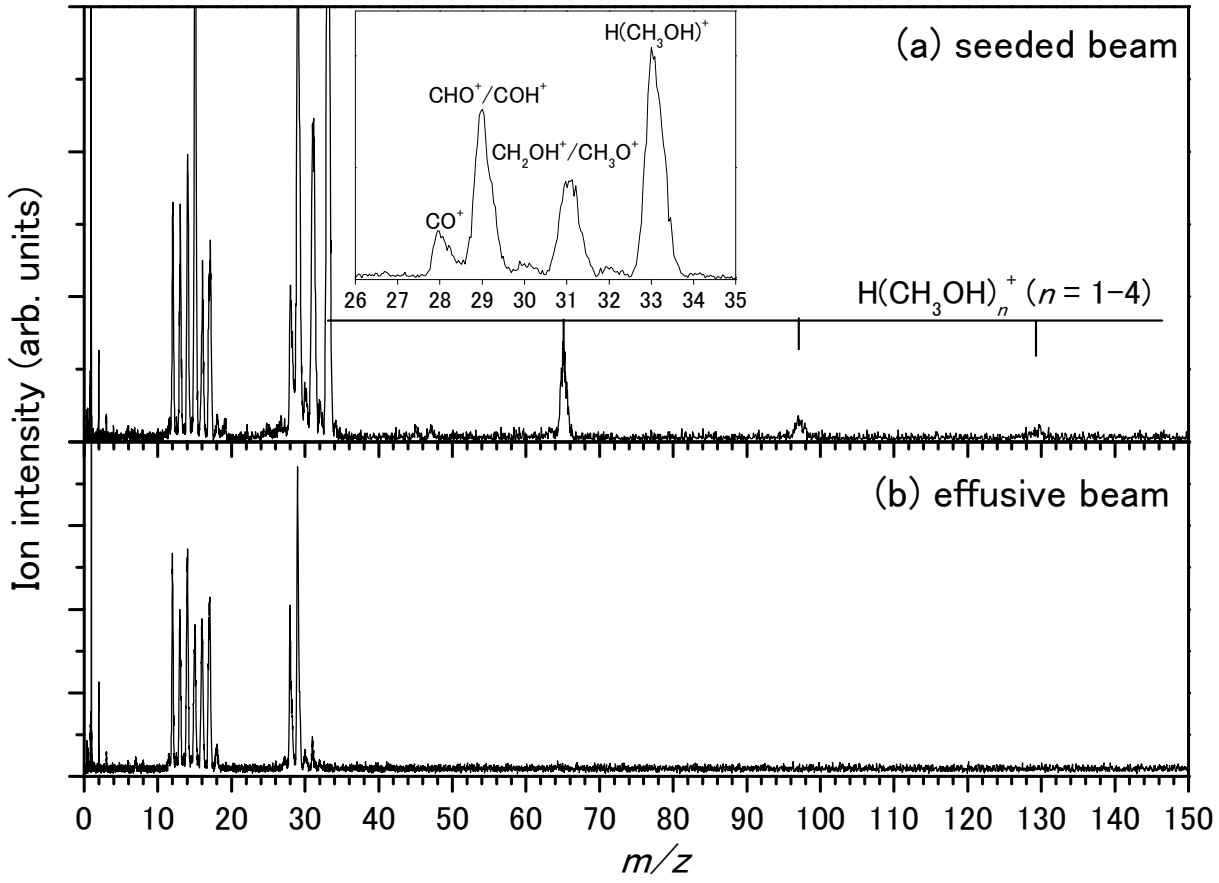
(a) seeded beam
(b) effusive beam
H(CH3OH)+
CHO+/COH+
CH2OH+/CH3O+
CO+
26 27 28 29 30 31 32 33 34 35
H(CH3OH)n+ (n = 1–4)
Ion intensity (arb. units)
0 10 20 30 40 50 60 70 80 90 100 110 120 130 140 150
m/z

Figure 2

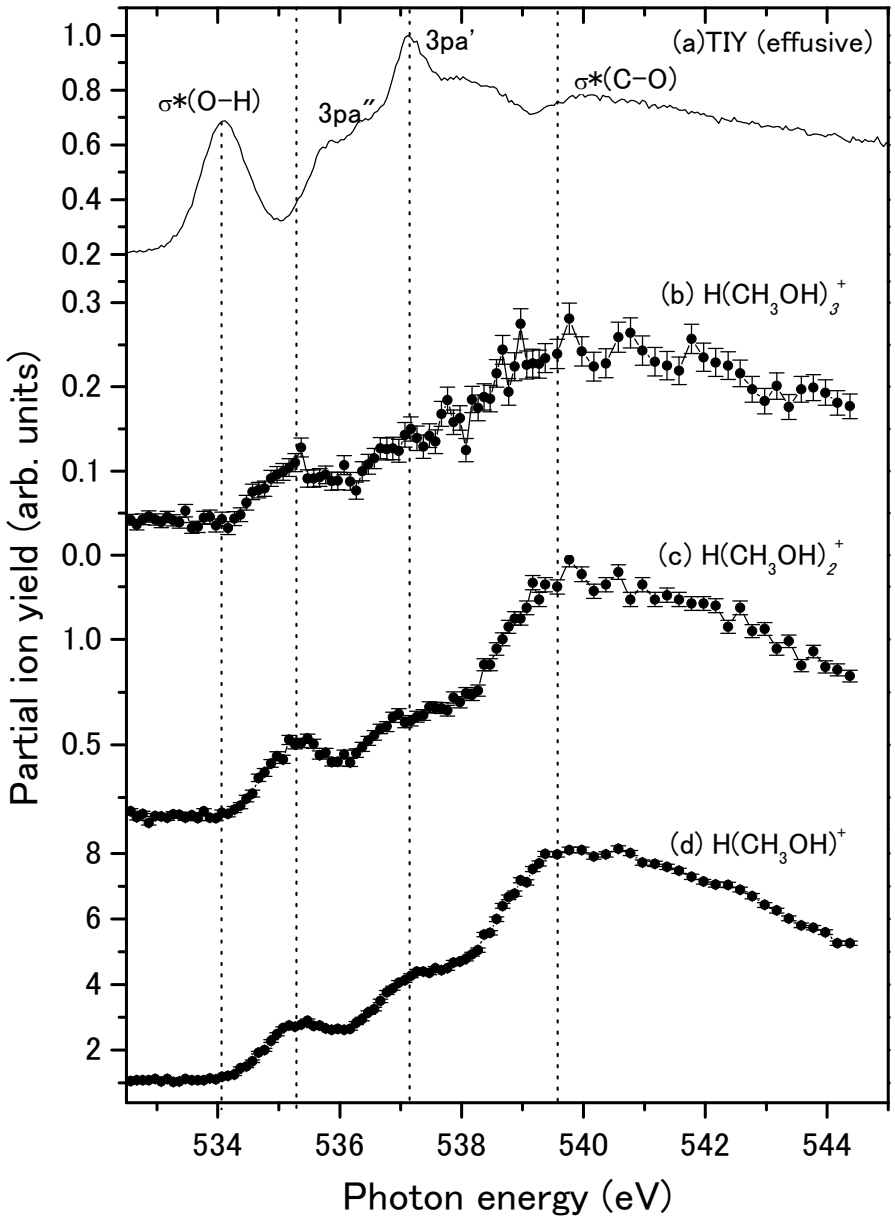
(a)TIY (effusive)
σ*(O–H)
3pa″
3pa'
σ*(C–O)
(b) H(CH3OH)3+
(c) H(CH3OH)2+
(d) H(CH3OH)+
Partial ion yield (arb. units)
Photon energy (eV)
534
536
538
540
542
544

Figure 3A

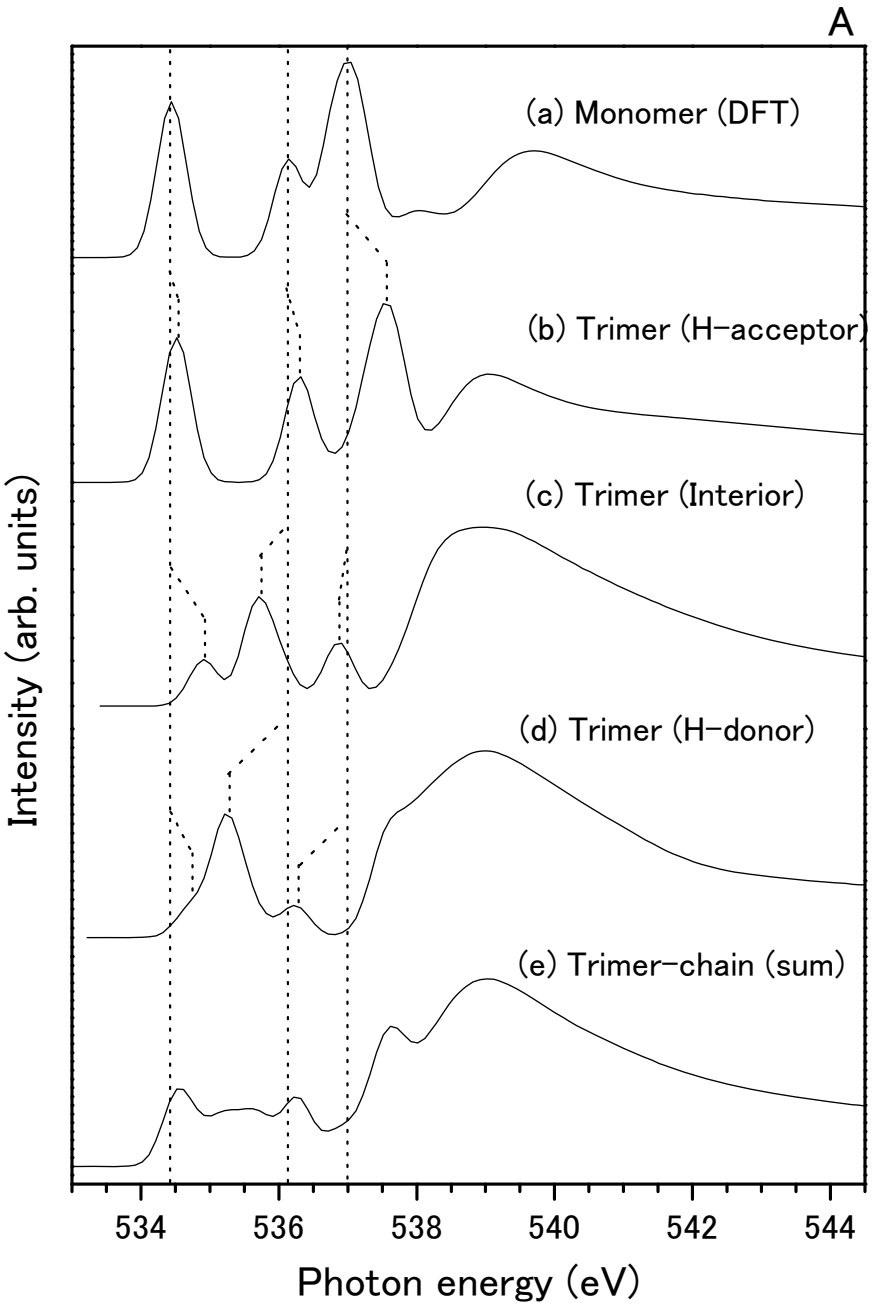
A
(a) Monomer (DFT)
(b) Trimer (H-acceptor)
(c) Trimer (Interior)
(d) Trimer (H-donor)
(e) Trimer-chain (sum)
Intensity (arb. units)
534
536
538
540
542
544
Photon energy (eV)

Figure 3B

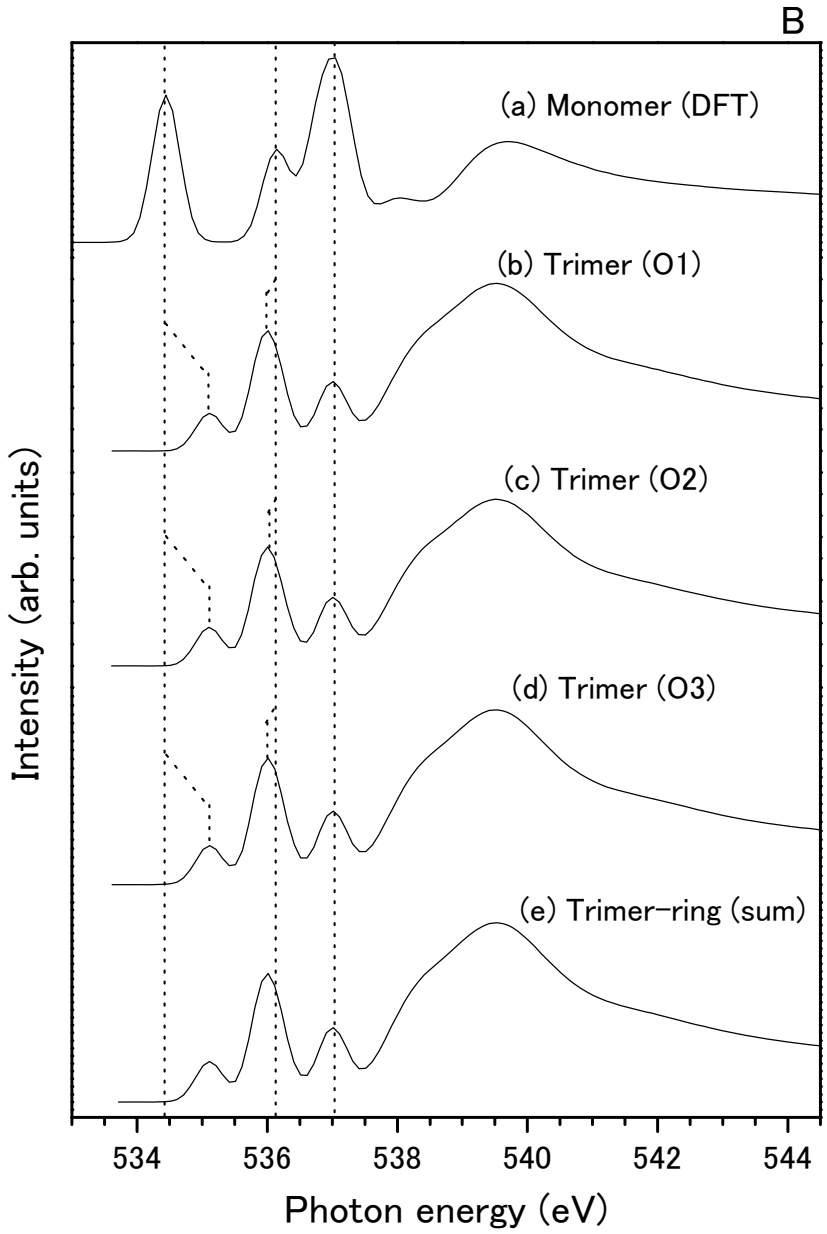
B
(a) Monomer (DFT)
(b) Trimer (O1)
(c) Trimer (O2)
(d) Trimer (O3)
(e) Trimer−ring (sum)
Intensity (arb. units)
534
536
538
540
542
544
Photon energy (eV)

Figure 4

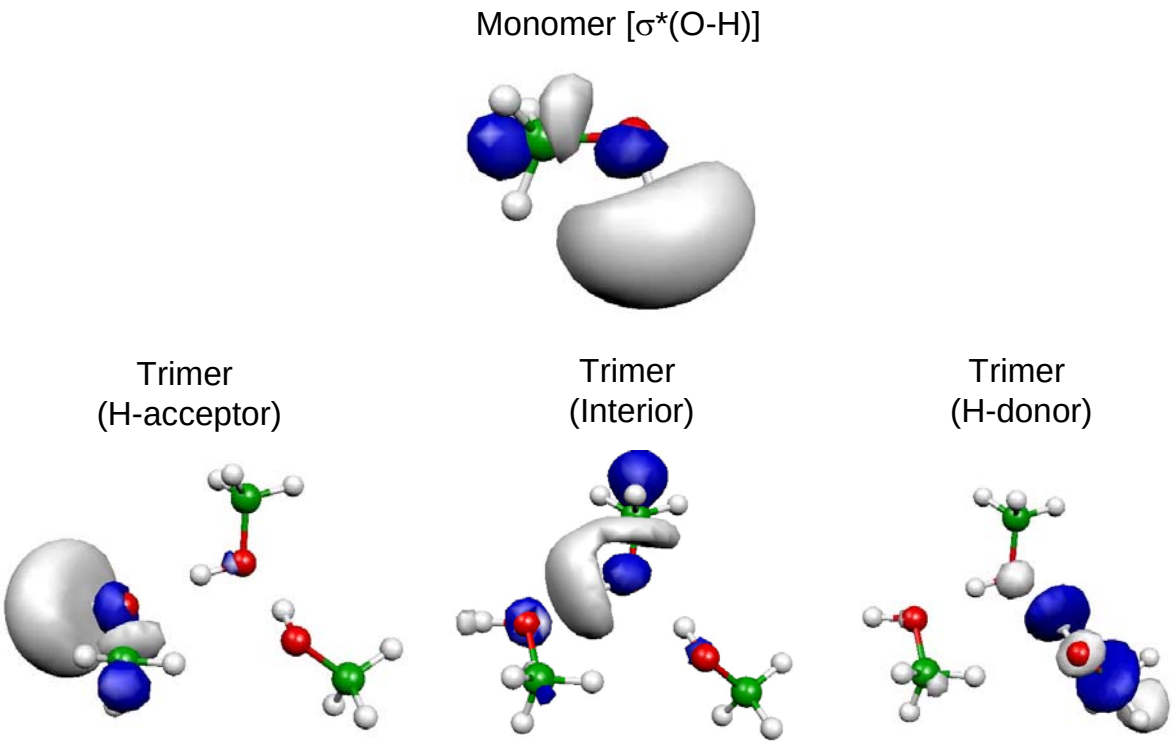
Monomer [σ*(O-H)]
Trimer
(H-acceptor)
Trimer
(Interior)
Trimer
(H-donor)

Figure 5

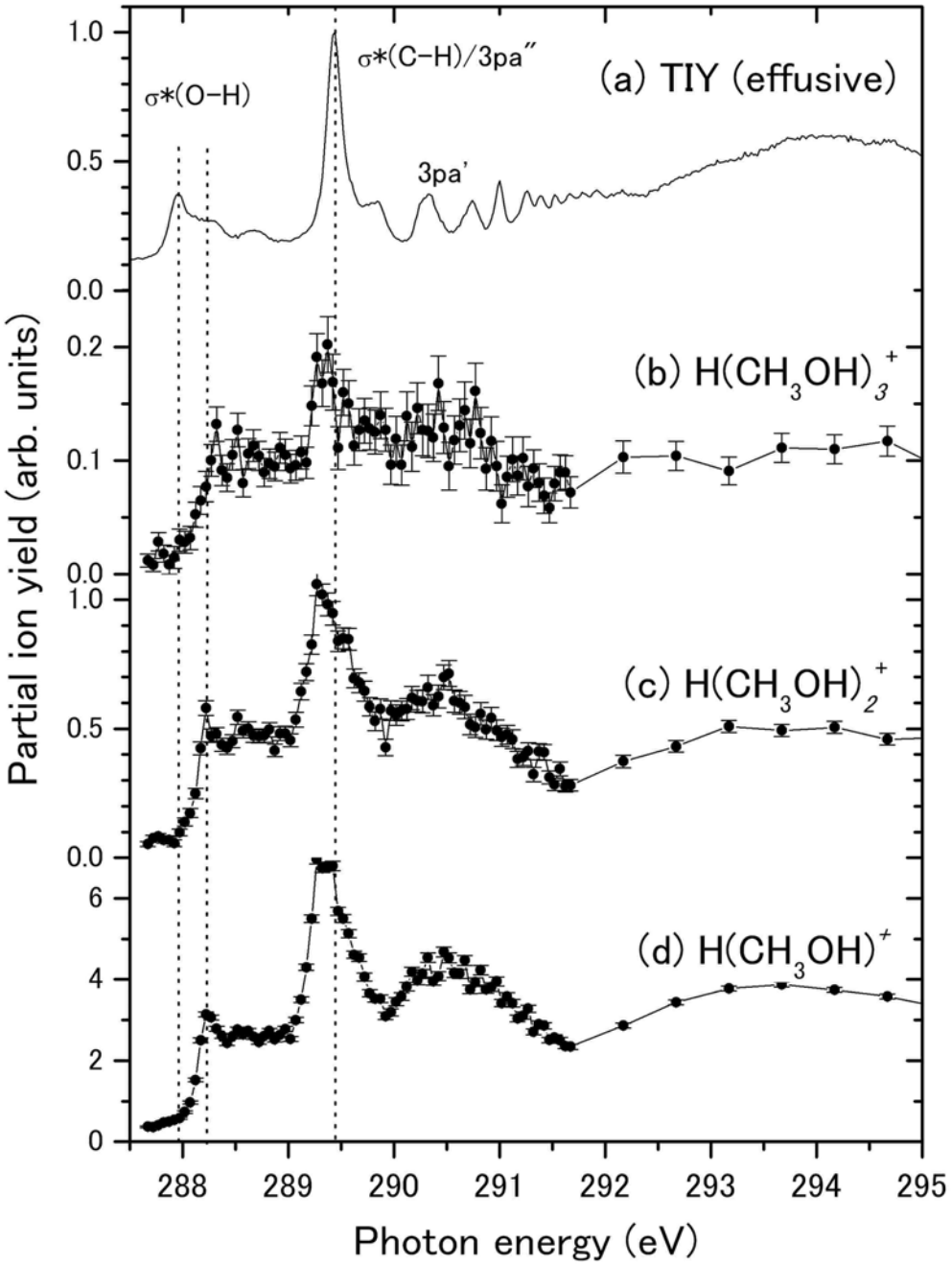
σ*(O-H)
σ*(C-H)/3pa″
3pa'
(a) TIY (effusive)
(b) H(CH3OH)3+
(c) H(CH3OH)2+
(d) H(CH3OH)+
Partial ion yield (arb. units)
Photon energy (eV)
1.0
0.5
0.0
0.2
0.1
0.0
1.0
0.5
0.0
6
4
2
0
288
289
290
291
292
293
294
295

Figure 6

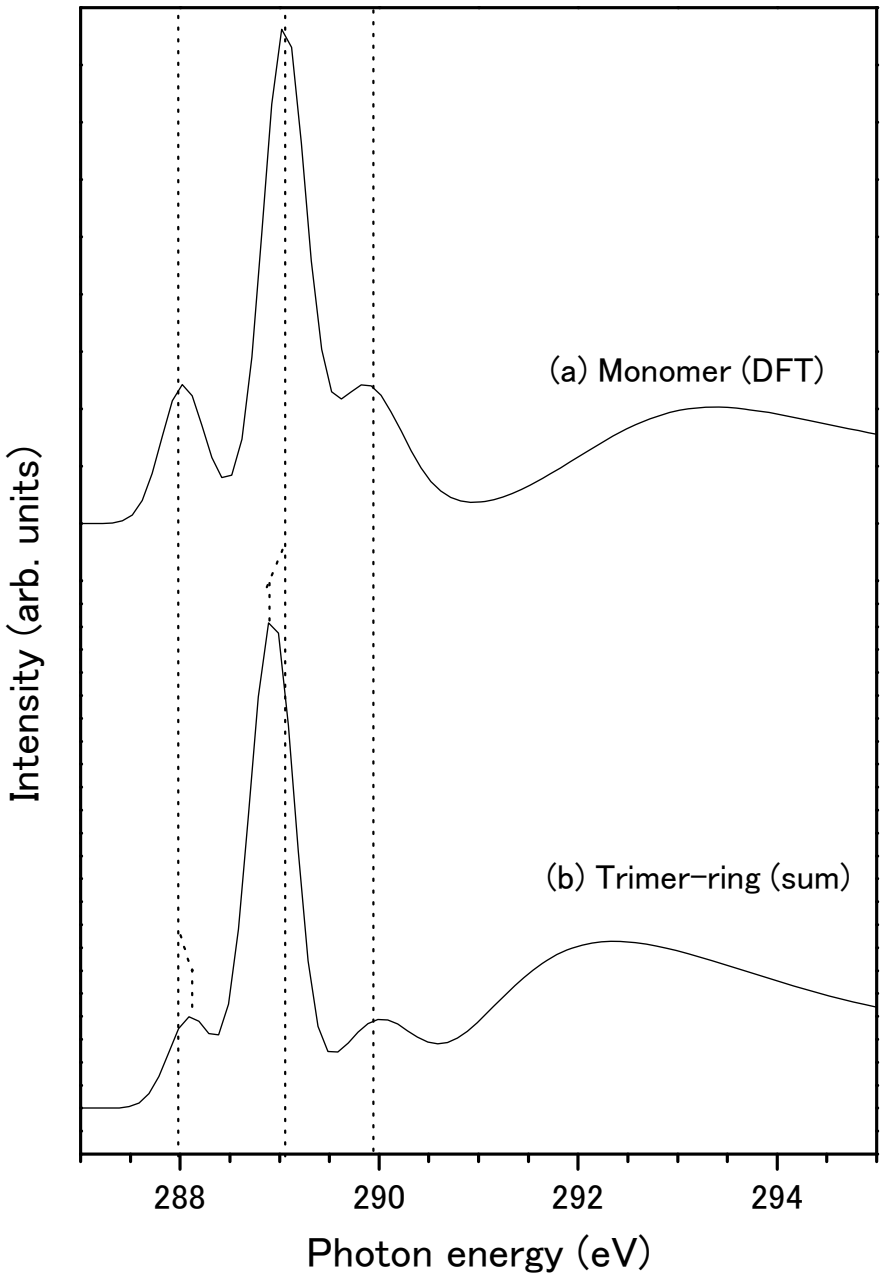
(a) Monomer (DFT)
(b) Trimer–ring (sum)
Intensity (arb. units)
288
290
292
294
Photon energy (eV)

References

[1] J. Stöhr, *NEXAFS Spectroscopy* (Springer-Verlag, Berlin, 1992).

[2] For example, E. Rühl, *Int. J. Mass Spectrom.* **229,** 117 (2003), and references therein.

[3] For example, L. A. Curtiss and M. Blander, *Chem. Rev.* **88,** 827 (1988).

[4] For example, D. Coulman, A. Puschmann, U. Höfer, H.-P. Steinrück, W. Wurth, P. Feulner, and D. Menzel, *J. Chem. Phys.* **93**, 58 (1990).

[5] J.-H. Guo, Y. Luo, A. Augustsson, J.-E. Rubensson, C. Såthe, H. Ågren, H. Siegbahn, and J. Nordgren, *Phys. Rev. Lett.* **89**, 137402 (2002).

[6] S. Myneni, Y. Luo, L. Å. Näslund, M. Cavalleri, L. Ojamäe, H. Ogasawara, A. Pelmenschikov, Ph. Wernet, P. Väterlein, C. Heske, Z. Hussain, L. G. M. Pettersson, and A. Nilsson, *J. Phys.: Condens. Matter* **14**, L213 (2002).

[7] M. Cavalleri, H. Ogasawara, L. G. M. Pettersson, and A. Nilsson, *Chem. Phys. Lett.* **364**, 363 (2002).

[8] K. R. Wilson, M. Cavalleri, B. S. Rude, R. D. Schaller, A. Nilsson, L. G. M. Pettersson, N. Goldman, T. Catalano, J. D. Bozek, and R. J. Saykally, *J. Phys: Condens. Matter* **14**, L221 (2002).

[9] Ph. Wernet, D. Nordlund, U. Bergmann, M. Cavalleri, M. Odelius, H. Ogasawara, L. Å. Näslund, T. K. Hirsch, L. Ojamäe, P. Glatzel, L. G. M. Pettersson, and A. Nilsson, *Science* **304**, 995 (2004).

[10] O. Björneholm, F. Federmann, S. Kakar, and T. Möller, *J. Chem. Phys.* **111,** 546 (1999).

[11] Y. Tamenori, T. Yamaguchi, K. Okada, K. Tabayashi, T. Gejo, and K. Honma, *J. Electron Spectrosc. Relat. Phenom.* **144–147,** 235 (2005).

[12] H. Ohashi, E. Ishiguro, Y. Tamenori, H. Okumura, A. Hiraya, H. Yoshida, Y. Senba, K. Okada, N. Saito, I. H. Suzuki, K. Ueda, T. Ibuki, S. Nagaoka, I. Koyano, and T. Ishikawa, *Nucl. Instrum. Meth. Phys. Res. A* **467,** 533 (2001); Y. Tamenori, H. Ohashi, E. Ishiguro, and T. Ishikawa, *Rev. Sci. Instrum.* **73,** 1588 (2002).

[13] T. Tanaka, X.-M. Marechal, T. Hara, T. Tanabe, and H. Kitamura, *J. Synchrotron Rad.* **5,** 459 (1998); T. Tanaka, T. Hara, M. Oura, H. Ohashi, H. Kimura, S. Goto, Y. Suzuki, and H. Kitamura, *Rev. Sci. Instrum.* **70,** 4153 (1999); T. Tanaka, M. Oura, H. Ohashi, S. Goto, Y. Suzuki, and H. Kitamura, *J. Appl. Phys.* **88,** 2101 (2000).

[14] A. Hiraya, Y. Senba, H. Yoshida, and K. Tanaka, *J. Electron Spectr. Relat. Phenom.* **101–103,** 1025 (1999); Y. Senba, H. Yoshida, T. Ogata, D. Sakata, A Hiraya, and K. Tanaka, *J. Electron Spectr. Relat. Phenom.* **101–103,** 131 (1999).

[15] J. Geiger and E. Rühl, *Int. J. Mass Spectrom.* **220,** 99 (2002).

[16] M. J. Frisch, G. W. Trucks, H. B. Schlegel, G. E. Scuseria, M. A. Robb, J. R. Cheeseman, J. A. M. Jr, T. Vreven, K. N. Kudin, J. C. Burant, J. M. Millam, S. S. Iyengar, J. Tomasi, V. Barone, B. Mennucci, M. Cossi, G. Scalmani, N. Rega, G. A. Petersson, H. Nakatsuji, M. Hada, M. Ehara, K. Toyota, R. Fukuda, J. Hasegawa, M. Ishida, T. Nakajima, Y. Honda, O. Kitao, H. Nakai, M. Klene, X. Li, J. E. Knox, H. P. Hratchian, J. B. Cross, C. Adamo, J. Jaramillo, R. Gomperts, R. E. Stratmann, O. Yazyev, A. J. Austin, R. Cammi, C. Pomelli, J. W. Ochterski, P. Y. Ayala, K. Morokuma, G. A. Voth, P. Salvador, J. J. Dannenberg, V. G. Zakrzewski, S. Dapprich, A. D. Daniels, M. C. Strain, O. Farkas, D. K. Malick, A. D. Rabuck, K. Raghavachari, J. B. Foresman, J. V. Ortiz, Q. Cui, A. G. Baboul, S. Clifford, J. Cioslowski, B. B. Stefanov, G. Liu, A. Liashenko, P. Piskorz, I. Komaromi, R. L. Martin, D. J. Fox, T. Keith, M. A. Al-Laham, C. Y. Peng, A. Nanayakkara, M. Challacombe, P. M. W. Gill, B. Johnson, W. Chen, M. W. Wong, C. Gonzalez, and J. A. Pople, Gaussian 03, Revision C.02 (Gaussian, Inc., Wallingford CT, 2004) (2004).

[17] K. Hermann, L. G. M. Pettersson, M. E. Casida, C. Daul, A. Goursot, A. Koester, E. Proynov, A. St-Amant, D. R. Salahub, V. Carravetta, H. Duarte, N. Godbout, J. Guan, C. Jamorski, M. Leboeuf, V. Malkin, O. Malkina, M. Nyberg, L. Pedocchi, F. Sim, L. Triguero, and A. Vela, StoBe-deMon version 1.0 (StoBe Software, 2002) (2002).

[18] O. Takahashi and L. G. M. Pettersson, *J. Chem. Phys.* **121**, 10339 (2004).

[19] O. Takahashi, K. Tabayashi, S. Wada, R. Sumi, K. Tanaka, M. Odelius, and L. G. M. Pettersson, *J. Chem. Phys.* **124**, 124901 (2006).

[20] O. Takahashi, S. Yamanouchi, K. Yamamoto, and K. Tabayashi, *Chem. Phys. Lett.* **419**, 501 (2006).

[21] L. Triguero, L. G. M. Pettersson and H. Ågren, *Phys. Rev.* **B58**, 8097 (1998).

[22] J. P. Perdew and Y. Wang, *Phys. Rev.* **B33**, 8800 (1986).

[23] J. P. Perdew and Y. Wang, *Phys. Rev.* **B45**, 13244 (1992).

[24] C. Kolczewski, R. Püttner, O. Plashkevych, H. Ågren, V. Staemmler, M. Martins, G. Snell, M. Sant'anna, G. Kaindl and L. G. M. Pettersson, *J. Chem. Phys.* **115**, 6426 (2001).

[25] L. G. M. Pettersson, U. Wahlgren and O. Gropen, *J. Chem. Phys.* **86**, 2176 (1987).

[26] K. C. Prince, R. Richter, M. de Simone, M. Alagia, and M. Coreno, *J. Phys. Chem. A* **107,** 1955 (2003).

[27] A. Hempelmann, M. N. Piancastelli, F. Heiser, O. Gessner, A. Rüdel, and U. Becker, *J. Phys. B: At. Mol. Opt. Phys.* **32,** 2677 (1999).

[28] Y. J. Shi, S. Consta, A. K. Das, B. Mallik, D. Lacey, and R. H. Lipson, *J. Chem. Phys.* **116,**

6990 (2002).

[29] S. Morgan and A. W. Castleman Jr., *J. Phys. Chem.* **93,** 4544 (1989).

[30] G. R. Wight and C. W. Brion, *J. Electron Spectros. Relat. Phenom.* **4,** 25 (1974).

[31] K. R. Wilson, M. Cavalleri, B. S. Rude, R. D. Schaller, T. Catalano, A. Nilsson, R. J. Saykally, and L. G. M. Pettersson, *J. Phys. Chem. B* **109,** 10194 (2005).

[32] Y. J. Hu, H. B. Fu, and E. R. Bernstein, *J. Chem. Phys.* **125**, 154306 (2006).

[33] F. Huisken, A. Kulcke, C. Laush, and J. M. Lisy, *J. Chem. Phys.* **95**, 3924 (1991); F. Huisken, M. Kaloudis, M. Koch, and O. Werhahn, *J. Chem. Phys.* **105**, 8965 (1996); U. Buck and B. Schmidt, *J. Chem. Phys.* **98**, 9410 (1993); U. Buck and I. Ettishcer, *J. Chem. Phys.* **108**, 33 (1998).

[34] M. Chergui, N. Schwentner, and W. Bohmer, *J. Chem. Phys.* **85**, 2472 (1986).

[35] S. Kashtanov, A. Augustson, J.-E. Rubensson, J. Nordgren, H. Agren, J.-H. Guo, and Y. Luo, *Phys. Rev. B* **71**, 104205 (2005).

[36] L.-Å. Näslund, J. Lüning, Y. Ufuktepe, H. Ogasawara, Ph. Wernet, U. Bergmann, L. G. M. Pettersson, and A. Nilsson, *J. Phys. Chem. B* **109**, 13835 (2005).

[37] O. Mó, M. Yánez, and J. Elguero, *J. Chem. Phys.* **107**, 3592 (1997).